Single-cycle multiterahertz transients with peak fields above 10 MV/cm

F. Junginger,[1] A. Sell,[1] O. Schubert,[1] B. Mayer,[1] D. Brida,[2] M. Marangoni,[2] G. Cerullo,[2] A. Leitenstorfer,[1] and R. Huber[1,*]

[1]Department of Physics and Center for Applied Photonics, University of Konstanz, Universitätsstrasse 10, 78464 Konstanz, Germany

[2]IFN-CNR, Dipartimento di Fisica, Politecnico di Milano, Piazza Leonardo da Vinci 32, 20133 Milano, Italy

*Corresponding author: rupert.huber@uni-konstanz.de

Received April 22, 2010; revised June 24, 2010; accepted June 24, 2010;
posted July 16, 2010 (Doc. ID 127306); published July 29, 2010

Phase-locked single-cycle transients with frequency components between 1 and 60 THz and peak fields of up to 12 MV/cm are generated as the idler wave of a parametric amplifier. To achieve broadband conversion in GaSe nonlinear crystals, we match the group velocities of signal and idler components. The influence of group-velocity dispersion is minimized by long-wavelength pumping at 1.18 μm. Free-space electro-optic sampling monitors the multiterahertz waveforms with direct field resolution. © 2010 Optical Society of America

OCIS codes: 190.4970, 190.2620, 320.7110, 320.7100, 120.5050.

Phase-stable sources of ultrabroadband terahertz (THz) transients between 1 and 100 THz have paved new avenues in fundamental science and technology [1,2]. In combination with field-sensitive detection [3–6], multi-THz pulses have been employed to probe low-energy elementary excitations in condensed matter with a subcycle temporal resolution [7–9]. Recently, THz nonlinear optical studies have created the need for elevated intensities [10–12]. Field amplitudes of up to 1 MV/cm have been achieved by free-electron lasers [13] and tabletop systems employing optical rectification (OR), i.e., difference frequency generation (DFG) between spectral components of a single broadband amplified laser pulse [14,15]. DFG between two distinct near-IR pulse trains with synchronized carrier-envelope phases has yielded widely tunable multi-THz fields of more than 100 MV/cm [16]. Yet strictly single-cycle pulses have not been demonstrated in this range. On the time scale of the oscillation period of light, nonlinear effects are expected to be sensitive to the absolute phase of the driving field. Intense single-cycle multi-THz transients are, therefore, highly desirable for THz control of low-energy elementary excitations, such as molecular vibrations [17] or electronic transitions in semiconductors [10–12] and strongly correlated systems [18], beyond the slowly varying envelope approximation.

Here we combine successful concepts of ultrabroadband optical parametric amplification (OPA) established in the near- and mid-IR spectral ranges [19–21] with recent high-field THz technology to generate phase-locked multi-THz transients in GaSe with frequency components covering close to six optical octaves. Peak electric fields of up to 12 MV/cm are obtained in a single oscillation cycle centered at 22 THz. Electro-optic detection maps out the temporal field trace with absolute amplitude and phase resolution.

GaSe has been known as an excellent material for broadband THz generation due to its exceptionally large nonlinear coefficient and infrared transparency. The strong birefringence allows for widely tunable phase matching. For a given set of pump, signal, and idler frequencies $(\omega_p, \omega_s, \omega_i)$, the phase-matching condition $\Delta k = k_p - k_s - k_i = 0$ can be fulfilled by tuning the internal propagation angle θ_{int}. While this interaction has been driven with pulses centered at $\lambda_p \approx 0.8$ μm as derived from Ti:sapphire lasers [3,4,15], pumping at longer wavelengths promises substantially shorter idler pulses: the broadest bandwidth is expected when the wave vector mismatch [22]

$$\Delta k \cong \left(\frac{\partial k_i}{\partial \omega_i} - \frac{\partial k_s}{\partial \omega_s}\right)\Delta\omega - \frac{1}{2}\left(\frac{\partial^2 k_i}{\partial \omega_i^2} + \frac{\partial^2 k_s}{\partial \omega_s^2}\right)\Delta\omega^2 + \ldots, \quad (1)$$

expanded in increasing orders of the frequency detuning $\Delta\omega$, reaches a minimum [19,20]. The first term describes group-velocity mismatch (GVM $= 1/v_{gi} - 1/v_{gs}$) of signal and idler pulses, while the second contribution accounts for group-velocity dispersion (GVD) at the signal and idler frequencies. To achieve the broadest phase-matching bandwidth, one needs to suppress the GVM and minimize the contribution of GVD. In a type I interaction and for a given pump frequency, one can always find a pair of signal and idler frequencies such that GVM $= 0$, provided that ω_s and ω_i are located on opposite sides of the zero-dispersion point. When this condition is met, the bandwidth is determined by the GVD, the minimization of which requires a favorable choice of the pump frequency. This fact is quantitatively illustrated in Fig. 1, which plots the phase-matching function $|\sin(\Delta kL)/(\Delta kL)|$ in a $\omega_i - \theta_{\mathrm{int}}$ plane for type I interaction in GaSe (thickness $L = 140$ μm) at $\lambda_p = 1.18$ μm [Fig. 1(a)] and 0.8 μm [Fig. 1(b)]. For each pump wavelength there exists a stationary point corresponding to group-velocity matching between signal and idler pulses, where the idler bandwidth is expected to be maximum. With $\lambda_p = 0.8$ μm, however, the phase-matching bandwidth is significantly lower due to much higher GVD of the idler. It exceeds the corresponding value for the 1.18 μm pump by approximately 1 order of magnitude.

To explore the bandwidth limitations of high-field THz generation, we start with a widely tunable source of intense near-IR pulses. The system is based on a hybrid concept, combining the stability of a multi-branch Er:fiber seed laser with the high pulse energies of a regenerative Ti:sapphire amplifier [16]. The latter provides 5 mJ pulses, at a repetition rate of 1 kHz, which pump two identical two-stage OPAs seeded by a shared white-light

0146-9592/10/152645-03$15.00/0

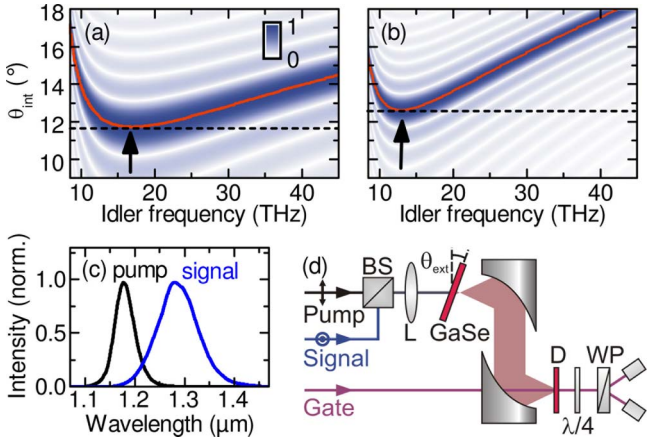

Fig. 1. (Color online) (a), (b) Phase-matching function $|\sin(\Delta kL)/(\Delta kL)|$ (color coded) as a function of the internal propagation angle θ_{int} and the idler frequency calculated for type I parametric amplification in GaSe ($L = 140$ μm). The pump wavelength is set to (a) 1.18 μm and (b) 0.8 μm. Red central curve, angle of perfect phase matching. Arrows, point of perfect group-velocity matching. (c) Spectra of near-IR pump and signal pulses employed in the experiment. The FWHM bandwidths amount to 45 and 90 nm, respectively. (d) Schematic setup of collinear parametric interaction and electro-optic detection. The pump polarization is set as extraordinary, while the signal and the idler are ordinary. The 1.2 μm gating pulse (duration, 8 fs) is generated by an Er:fiber laser that is optically synchronized to the near-IR OPAs. D, GaSe sensor (thickness, 30 μm); $\lambda/4$, waveplate; WP, Wollaston prism. The pump and signal waves are mutually phase coherent to warrant a stable carrier-envelope phase of the emerging idler transient.

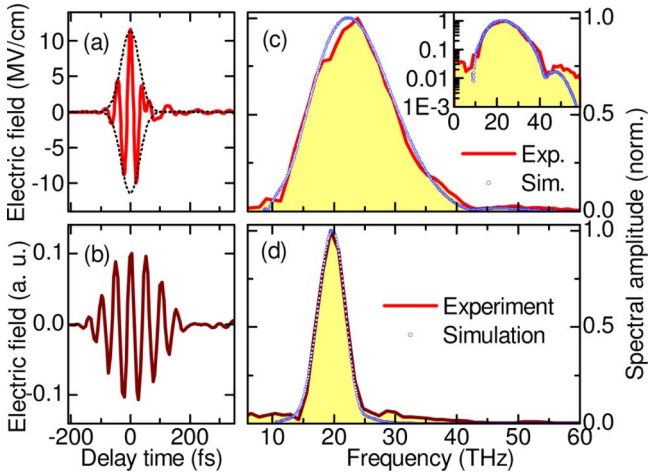

Fig. 2. (Color online) (a) Single-cycle idler pulse generated by parametric mixing of mutually phase coherent pump and signal waves centered at 1.18 and 1.28 μm, respectively; solid curve, field profile; dotted curves, amplitude envelope. (b) Multi-THz transient from OR of a 10 fs pulse centered at 800 nm. The field is uncalibrated since a low pump energy of 10 nJ is used in this case. Both waveforms (a) and (b) are detected in a 30-μm-thick GaSe electro-optic sensor. (c) Amplitude spectrum (FWHM, 15 THz) of the transient of panel (a). Inset, logarithmic plot of the spectra revealing frequency components over six optical octaves from 1 to 60 THz. (d) Amplitude spectrum (FWHM, 5 THz) corresponding to panel (b). Circles, numerical simulations.

continuum. One OPA is equipped with two type I β-barium borate (BBO) crystals. It generates 90-nm-wide signal spectra with a center wavelength of 1.28 μm [Fig. 1(c)] and a pulse energy of 150 μJ. After compression in a pair of SF10 glass prisms, a temporal width of less than 30 fs is measured. The second OPA is operated with two type II BBO crystals and provides pump pulses at a center wavelength of 1.18 μm with a 360 μJ energy and a 45 nm FWHM bandwidth [Fig. 1(c)]. The pump pulse duration of 115 fs would allow for an interaction length up to 10 mm thanks to the very low GVM between pump and signal/idler pulses (10 fs/mm). As depicted in Fig. 1(d), pump and signal pulses are collinearly superimposed in a polarizing beam splitter and focused into a GaSe crystal for type I mixing. The carrier-envelope offset frequency of the emerging idler wave is expected to be inherently locked to zero due to the mutual phase coherence of pump and signal [16,23]. The THz radiation is finally focused onto a 30-μm-thick GaSe detector, where the field trace is mapped out electro-optically [3–6,15,16]. The 8 fs gate pulse used for this purpose is derived from the multi-branch Er:fiber laser, which is passively synchronized to the regenerative Ti:sapphire amplifier [5,16].

Figure 2(a) shows the temporal form of an idler wave generated in a 140-μm-long GaSe crystal at $\theta_{\text{int}} = 12.5°$, i.e., close to group-velocity matching. The phase-locked transient features a single dominant field maximum. The FWHM of the intensity envelope is found to be 46 fs, corresponding to exactly 1.0 cycles of the carrier wave at the center frequency of 22 THz. In comparison, typical THz pulses from OR of 10 fs pump pulses centered at a wavelength of 800 nm in the same emitter crystal are longer by a factor of 3 (FWHM, 140 fs) [Fig. 2(b)], in good agreement with the expected scaling of the phase-matching bandwidth with the square root of GVD. In Fig. 2(a), we do not observe OR of the pump or signal alone, because they are not phase matched. The energy contained in the single-cycle transient amounts to 0.4 μJ, as measured with a calibrated thermopile detector, corresponding to a conversion efficiency of 3%. From the focal diameter of 55 μm, we retrieve a peak electric field of 12 MV/cm. This result represents by far the most intense phase-stable single-cycle THz transient known to us.

The corresponding amplitude spectrum exhibits a broad peak at 22 THz with a FWHM extending from 15 to 30 THz [Fig. 2(c)]. Frequency components covering almost six optical octaves between 1 and 60 THz are discernible far above the noise floor [inset of Fig. 2(c)]. A weak dip in the range from 7 to 10 THz is due to optical phonon resonances in the emitter. The measured spectrum agrees well with a numerical simulation accounting for the full time-dependent nonlinear propagation equations of the OPA process between 10 and 60 THz [22]. This calculation also reproduces the side maximum at 48 THz. In contrast, the width of the THz spectrum obtained by OR of 800 nm pulses is narrower by a factor of 3 [Fig. 2(d)], in agreement with the simulations carried out according to the model reported in [24].

The group-velocity-matched interaction allows for ultrashort multi-THz transients to be generated also in rather long mixing crystals. Figure 3(a) displays a set of phase-stable idler waves obtained with GaSe elements of various lengths. All pulses generated with $L \leq 460$ μm

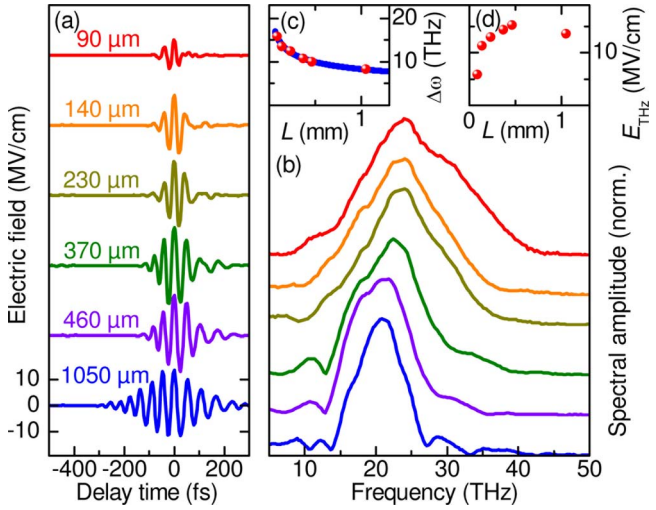

Fig. 3. (Color online) (a) Transients and (b) corresponding amplitude spectra from GaSe crystals with varying length L as indicated to the left. (c) Bandwidth $\Delta\omega$ of the measured amplitude spectra (circles) as a function of L. Solid curve, numerical fit of $L^{-1/4}$ dependence due to residual GVD mismatch. (d) Peak electric fields as a function of L.

contain less than two optical cycles within their FWHM. A 90-μm-thick crystal even affords transients as short as 42 fs. The corresponding spectra of the THz pulses are reported in Fig. 3(b). Their FWHM [Fig. 3(c)] remarkably exhibits a weak thickness dependence following an $L^{-1/4}$ law, as expected for a group-velocity-matched OPA [22]. In the temporal domain, the pulse widths do not follow the same law due to the GVD experienced by the idler pulse. The negative sign of the GVD results in a slight down-chirp, clearly discernible in the time traces for the longer crystals. The field amplitude increases with L to reach a saturation value of 15 MV/cm for $L =$ 460 μm [Fig. 3(d)].

In conclusion, we have demonstrated and characterized an intense source of inherently phase-locked single-cycle multi-THz transients with amplitudes above 10 MV/cm. The high peak field, which is concentrated in a single oscillation of the carrier wave, makes these pulses ideally suited for applications in extreme nonlinear optics and spectroscopy beyond the slowly varying envelope approximation, such as high-harmonics generation and field-resolved photon echo experiments throughout the mid-IR.

This work has been supported by the Emmy Noether Program of the Deutsche Forschungsgemeinschaft (DFG) and by the U. S. Air Force Office of Scientific Research (AFOSR) (grant FA8655-09-1-3101).

References

1. B. Ferguson and X.-C. Zhang, Nat. Mater. **1**, 26 (2002) and references therein.
2. M. Tonouchi, Nat. Photon. **1**, 97 (2007) and references therein.
3. C. Kübler, R. Huber, S. Tübel, and A. Leitenstorfer, Appl. Phys. Lett. **85**, 3360 (2004).
4. K. Liu, J. Xu, and X.-C. Zhang, Appl. Phys. Lett. **85**, 863 (2004).
5. A. Sell, R. Scheu, A. Leitenstorfer, and R. Huber, Appl. Phys. Lett. **93**, 251107 (2008).
6. T. Kampfrath, J. Nötzold, and M. Wolf, Appl. Phys. Lett. **90**, 231113 (2007).
7. R. Huber, F. Tauser, A. Brodschelm, M. Bichler, G. Abstreiter, and A. Leitenstorfer, Nature **414**, 286 (2001).
8. J. Kröll, J. Darmo, S. S. Dhillon, X. Marcadet, M. Calligaro, C. Sirtori, and K. Unterrainer, Nature **449**, 698 (2007).
9. G. Günter, A. A. Anappara, J. Hees, A. Sell, G. Biasiol, L. Sorba, S. De Liberato, C. Ciuti, A. Tredicucci, A. Leitenstorfer, and R. Huber, Nature **458**, 178 (2009).
10. B. E. Cole, J. B. Williams, B. T. King, M. S. Sherwin, and C. R. Stanley, Nature **410**, 60 (2001).
11. J. R. Danielson, Y.-S. Lee, J. P. Prineas, J. T. Steiner, M. Kira, and S. W. Koch, Phys. Rev. Lett. **99**, 237401 (2007).
12. S. Leinss, T. Kampfrath, K. V. Volkmann, M. Wolf, J. T. Steiner, M. Kira, S. W. Koch, A. Leitenstorfer, and R. Huber, Phys. Rev. Lett. **101**, 246401 (2008).
13. G. L. Carr, M. C. Martin, W. R. McKinney, K. Jordan, G. R. Neil, and G. P. Williams, Nature **420**, 153 (2002).
14. K.-L. Yeh, M. C. Hoffmann, J. Hebling, and K. A. Nelson, Appl. Phys. Lett. **90**, 171121 (2007).
15. K. Reimann, R. P. Smith, A. M. Weiner, T. Elsaesser, and M. Woerner, Opt. Lett. **28**, 471 (2003).
16. A. Sell, A. Leitenstorfer, and R. Huber, Opt. Lett. **33**, 2767 (2008).
17. M. L. Cowan, B. D. Bruner, N. Huse, J. R. Dwyer, B. Chugh, E. T. J. Nibbering, T. Elsaesser, and R. J. D. Miller, Nature **434**, 199 (2005).
18. M. Rini, R. Tobey, N. Dean, J. Itatani, Y. Tomioka, Y. Tokura, R. W. Schoenlein, and A. Cavalleri, Nature **449**, 72 (2007).
19. D. Brida, G. Cirmi, C. Manzoni, S. Bonora, P. Villoresi, S. De Silvestri, and G. Cerullo, Opt. Lett. **33**, 741 (2008).
20. D. Brida, M. Marangoni, C. Manzoni, S. De Silvestri, and G. Cerullo, Opt. Lett. **33**, 2901 (2008).
21. A. Gambetta, R. Ramponi, and M. Marangoni, Opt. Lett. **33**, 2671 (2008).
22. G. Cerullo and S. De Silvestri, Rev. Sci. Instrum. **74**, 1 (2003).
23. C. Manzoni, M. Först, H. Ehrke, and A. Cavalleri, Opt. Lett. **35**, 757 (2010).
24. R. A. Kaindl, F. Eickemeyer, M. Woerner, and T. Elsaesser, Appl. Phys. Lett. **75**, 1060 (1999).